Improvement of Processability of Clay/Polylactide Nanocomposites by a Combinational Method: *In Situ* Polymerization of L-Lactide and Melt Compounding of Polylactide

Seongnam Lee,[1] Chang-Hyeon Kim,[2] Jung-Ki Park[1]

[1]*Department of Chemical and Biomolecular Engineering,Korea Advanced Institute of Science and Technology, 373-1, Kuseong-dong, Yuseong-gu, Daejon, 305-701, Republic of Korea*
[2]*The 2nd Research Laboratory, Daeduk Research Institute of Honam Petrochemical Corporation, 24-1 Jang-dong, Yuseong-gu, Daejeon, 305-726, Republic of Korea*

Received 9 September 2004; accepted 7 April 2005
DOI 10.1002/app.22438
Published online in Wiley InterScience (www.interscience.wiley.com).

ABSTRACT: A modified clay/polylactide nanocomposite was prepared. The clay was modified by grafting polylactide chains onto the surface of clay. The modified clay was melt-compounded with a high-molecular-weight polylactide matrix. This novel clay/polylactide nanocomposite showed high shear-thinning behavior when the molecular weight of the grafted poly(L-lactide) was rather high. © 2006 Wiley Periodicals, Inc. J Appl Polym Sci 101: 1664–1669, 2006

Key words: polylactide; clay; ring-opening polymerization; nanocomposites

INTRODUCTION

The use of polylactide (PL), which is a biocompatible and biodegradable polymer, has been mainly focused on its application to a matrix for drug delivery systems,[1] tissue engineering,[2] and medical sutures.[3] Recently, PL also has been considered an environmentally friendly material because of its biodegradability and high mechanical strength that could be used as an alternative to commodity plastics such as polyethylene, polypropylene, and polystyrene.[4] However, the poor processability and barrier properties and also the rigid mechanical property of PL often limit its applicability. Previous studies on the processibility of PL reported on the low shear thinning[5] and degradation of PL during melt processing.[6]

To enhance the shear-thinning, thermal stability, and barrier properties of PL, trials have been performed to introduce silicates to the PL matrix using two methods: melt compounding of pure PL with clay[8] and *in situ* polymerization of lactide monomer in the presence of simply modified clay and a ring-opening catalyst.[9] The melt-compounding method can increase complex viscosity in a low-frequency range, which results in higher shear thinning of the nanocomposite as compared with pure PL. There have been no reports on the rheological properties of *in situ* polymerized products. The reported rheological behavior of end-tethered polycaprolactone onto the surface of layered silicate nanocomposite may provide some insight into the rheological behavior of the product of *in situ* polymerization.[10] End-tethered polycaprolactone showed nonterminal behavior in a low-frequency range, even with a low clay content.

In contrast, with the simply modified clay/PL composite obtained by the melt-compounding method, a higher clay content of around 5–7 wt % is needed to accomplish high shear thinning comparable to that with polypropylene. Though it might be rather easier to achieve higher shear thinning even with a lower clay content in the simply modified clay/PL composite by *in situ* polymerization of the lactide monomer, it was expected that it would be difficult to obtain a high-molecular-weight PL matrix in the silicate region from a heterogeneous reaction, which would limit its applicability because of poor mechanical strength.

It thus was anticipated that higher shear thinning and sufficient mechanical strength of the nanocomposite could be achieved at a lower clay content by melt compounding of the end-tethered PL with a high-molecular-weight PL matrix. Therefore, in this study, we first prepared the end-tethered polylactide nanocomposite and then melt-compounded it with high-molecular-weight PL. We investigated the effect

Correspondence to: Jung-Ki Park (jungpark@kaist.ac.kr)
Contract grant sponsor: Honam Petrochemical Corporation.
Contract grant sponsor: Brain Korea 21 Project.

TABLE I
Reaction Conditions of *In Situ* Graft Polymerization of L-Lactide onto a Clay Surface

Code	L-Lactide (g)	Cloisite® 30B (g)	Catalyst[a] (mmol)	Solvent[b] (mL)	Reaction temperature (°C)	Reaction time (day)
Clay-*g*-PLL01	43.2	4.32	3.9	240	135	3
Clay-*g*-PLL02	43.2	4.32	0.3	240	135	7

[a] Tin(II) octoate.
[b] Xylene.

of the chain length of poly(L-lactide) (PLL) grafted onto the surface of clay on the processability of the composite. The microstructures of the nanocomposite also were characterized.

EXPERIMENTAL

Materials

Commercial-grade PL, a Cargill-Dow product (Minneapolis, MN), was characterized by gel permeation chromatography, differential scanning calorimetry, and polarimetry: weight-average molecular weight = 190,000 g/mol, polydispersity index = 2.3, glass-transition temperature = 61°C, melting temperature = 152°C, and D-lactide content = 6.6 wt %. L-Lactide was purchased from Aldrich and recrystallized 3 times from dried toluene. Cloisite® 30B, an organically modified clay with bis(2-hydroxyethyl)methyl tallow-alkyl ammonium cations, was purchased from Southern Clay Products (Gonzales, TX) and dried in vacuum at 70°C for 1 day prior to use. The amount of organic modifier in Cloisite® 30B, determined with a thermal gravity analyzer, was found to be about 27 wt %. Tin(II) octoate was purchased from Aldrich (Milwaukee, WI) and distilled before use in the reaction. Xylene was purchased from Junsei (Tokyo, Japan) and distilled with sodium metal. All other chemicals were reagent grade and used without further purification.

In situ polymerization of L-lactide

For the *in situ* polymerization of L-lactide at the clay surface, the hydroxyl groups at the clay surface were activated by tin(II) octoate[11] for 1 day in the presence of xylene at 50°C in a glove box. After activation was accomplished, L-lactide was added to the mixture in a round-bottomed flask, and the reaction temperature was raised to 135°C for insertion-coordination ring-opening polymerization. With a preset time, the product was precipitated in diethyl ether and was dispersed in tetrahydrofuran for centrifugation. The precipitant was dried in vacuum at 70°C for 1 day.

Melt compounding of high-molecular-weight PL with PLL-grafted clay

PLL grafted onto a clay surface (clay-*g*-PLL) was compounded with high-molecular-weight commercial-grade PL by a Brabender mixer. With a predetermined ratio of clay-*g*-PLL to high-molecular-weight PL, the compounding procedure was performed at a constant mixing speed, 40 rpm, at 180°C for 15 min. For comparative studies, the PL also was compounded with Cloisite® 30B in the same experimental conditions as above.

Characterization

The PLL content in the synthesized clay-*g*-PLL was determined with a thermal gravity analyzer, TGA Q500 (TA Instrument) in the temperature range of 30°C–300°C in a nitrogen atmosphere. The molecular weight of PLL in the synthesized clay-*g*-PLL was determined by gel permeation chromatography (Waters 410 differential refractometer, Waters™ 600 pump). The clay-*g*-PLL underwent an ion-exchange reaction with a 0.1*M* LiCl solution in tetrahydrofuran in order to extract the grafted PLL. Microstructure analysis was performed by XRD (D/MAX-IIIC, RIGAKU). The intensity of X-ray distribution was measured at ambient temperature in the range of diffraction angle (2θ) from 1.2° to 30°, with a scanning rate of 1°/min on a diffractometer with CuKα radiation. The morphology also was checked by TEM (Tecnai F20) using an acceleration voltage of 100 kV. Ultrathin sections of the composites were cut at −130°C with a Reichert ultracryomicrotome equipped with a diamond knife. Rheological measurements were done by an ARES rotational rheometer (Rheometric Scientific) with a 25-mm parallel plate in a 1-mm gab. The measurements proceeded under conditions of a 10% constant strain in a dynamic frequency sweep mode at 210°C.

RESULTS AND DISCUSSION

Synthesis of clay-g-PLL

The reaction conditions and results of *in situ* graft polymerization of L-lactide onto the clay surface are shown in Tables I and II. In the *in situ* graft polymerization, the clay-*g*-PLL was recovered from the reaction product by centrifugation. Table II shows that the product yield was more than 99 wt %, indicating that the L-lactide monomers were almost completely converted to PLL grafted onto the clay surface. It also can be seen from Table II that the clay content of the

TABLE II
Reaction Results of *In Situ* Graft Polymerization of L-Lactide onto a Clay Surface

Code	Calculated clay content[a] (wt %)	Clay content[b] (wt %)	M_n of PLL[c] (g/mol)	PDI	Product yield (wt %)
Clay-*g*-PLL01	10	9.7	9400	1.25	>99
Clay-*g*-PLL02	10	9.6	21600	1.42	>99

[a] Calculated from feed weight ratio of Cloisite® 30B to L-lactide.
[b] Measured by TGA.
[c] Measured by GPC using polystyrene standard.
[d] Measured after centrifugation three times and vacuum drying.

centrifuged product was nearly the same as the calculated clay content from the feed composition, indicating that an almost complete grafting reaction took place at the clay surface during the *in situ* polymerization. The number-average molecular weight of the grafted PLL was found to be 9400 and 21,600 for clay-*g*-PLL01 and clay-*g*-PLL02, respectively. The polydispersity indices of these two grafted PLLs were rather low. This was because of restricted mobility of the growing chains confined between the silicate layers, which were able to prevent transesterification side reactions.[12] These two different clay-*g*-PLLs were comparatively studied in order to understand the effect of grafted PLL chain length on the rheological behavior of the nanocomposite.

Microstructure of melt-compounded clay-*g*-PLL/PL and clay/PL

The contents of clay-*g*-PLL, cloisite (R) 30B, and PL used in the melt compounding are shown in Table III. Figure 1 shows the TEM images of the melt-compounded nanocomposites. In the TEM images, disordered, intercalated, or nearly exfoliated structures[14] of clay-*g*-PLL/PL and clay/PL can be observed. As shown in Figure 2, the WAXD patterns, which do not appear to have peaks corresponding to the clay interspacing ($2\theta = 4.8$), also support the TEM results.

Rheological property of clay-*g*-PLL/PL

The effect of PLL chain length on the processability of the melt-compounded clay-*g*-PLL/PL nanocomposite is shown in Figures 3 and 4. From Figure 3(a), it can be seen that the complex viscosity of clay-*g*-PLL01/PL (M_n of grafted PLL = 9400 g/mol) generally decreased with an increase in PLL content, indicating that the dominant role of clay-*g*-PLL01 was as an internal plasticizer. Although the clay-*g*-PLL01 had an end-tethered structure, the short chain length of PLL was rather difficult to entangle with chains of the PL matrix so that PLL simply acted as an internal plasticizer. In fact, the critical molecular weight of chain entanglement of PLL is known to be about 9000 g/mol.[15–17] Thus, the end-tethered effect of the clay-*g*-PLL01 in the PL matrix was offset by the low molecular weight of the PLL chains. Support for this explanation also was provided by the storage and loss modulus data. Figure 3(b,c) displays the storage and loss modulus curves of clay-*g*-PLL01/PL. At first, it was noted that the storage modulus of clay-*g*-PLL01/PL was lower than that of pure PL over the entire frequency range. This is because chain entanglement of pure PL was much more effective than that in clay-*g*-PLL01/PL. With an increasing clay content of the nanocomposite, a transition in storage modulus behavior was observed in the frequency region of around 10 rad/s. When the frequency was below about 10 rad/s, the storage modulus increased with an increase in clay content. However, in the region above a frequency of 10 rad/s, the storage modulus decreased with an increase in clay content. This rheological behavior can be understood by the dispersion of clay in nanocomposites and also by chain slippage. As shown in Figures 1(a) and 2, the microstructure of the clay-*g*-PLL01/PL nanocomposite prepared in this study was disordered, intercalated, or nearly exfoliated. This well-dispersed state

TABLE III
Compounding Conditions of Clay-*g*-PLL/PL and Clay/PL

Code	Type of clay	Clay content (wt %)	Mixer speed (rpm)	Mixing time (min)	Mixing temperature (°C)
Clay-*g*-PLL01/PL[a]	Clay-*g*-PLL01	0.5, 1, 3[b]	40	15	180
Clay-*g*-PLL02/PL[a]	Clay-*g*-PLL02	0.5, 1, 3[b]	40	15	180
Clay/PL[a]	Cloisite® 30B	1, 3	40	15	180

[a] Cargill-Dow polylactide
[b] Weight percents (wt %) of clay-*g*-PLL are 5, 10, and 30, respectively.

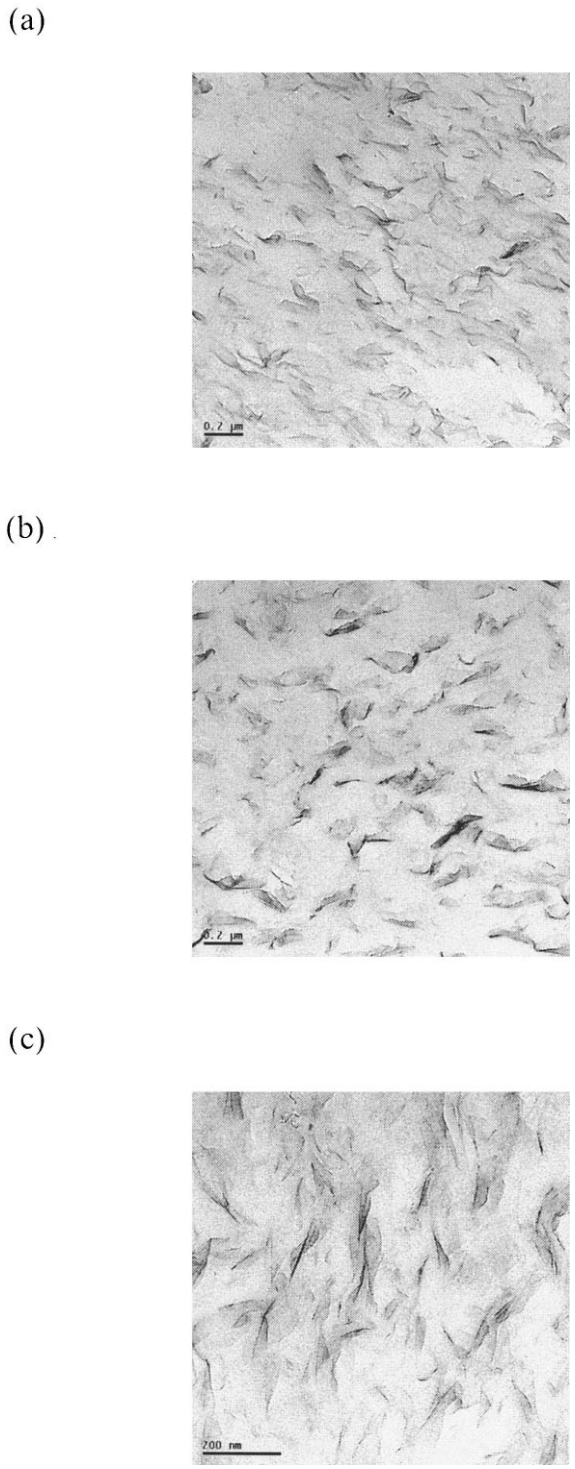

Figure 1 TEM images of clay-*g*-PLL/PL and clay/PL nanocomposite (3 wt % clay): (a) clay-*g*-PLL01/PL, (b) clay-*g*-PLL02/PL, (c) clay/PL.

may mimic a lower-frequency state. As the frequency becomes higher, a higher orientations of the clay will develop. At this stage of shear stress, the elasticity of the nanocomposite would be affected significantly by interactions between the grafted PLL chains on the clay surface and the chains of the matrix. In a certain frequency range, chain slippage may be induced by low-molecular-weight PLL chains. Thus, a transition in storage modulus behavior could be observed. These plasticizing effects were more obvious in the loss modulus behavior of clay-*g*-PLL01/PL. It was clearly represented in the loss modulus behavior—the modulus decreased with an increase in clay content.

Figure 4(a) shows that for the clay-*g*-PLL02/PL (M_n of grafted PLL = 21,600 g/mol), the dominant role of the clay-*g*-PLL02 in the composite was to enhance viscosity, especially with a clay content of around 3 wt %. The storage and loss moduli of clay-*g*-PLL02/PL are shown in Figure 4(b,c). From the storage modulus results, it is apparent that the nonterminal behavior occurred in the low-frequency range and was more significant with increased clay content. This nonterminal behavior resulted from the end-tethered structure of clay-*g*-PLL, which was reported previously.[10] The molecular weight of the PLL of clay-*g*-PLL02 was above the critical molecular weight of entanglement of PLL, and thus the PLL chains could effectively entangle with the chains of the PL matrix. Above a frequency of about 50 rad/s, storage modulus decreased with clay content. In this frequency region, the shear stress seemed to be high enough to disentangle the PLL chains from the chains of PL matrix; thus, the plasticizing effect of chain slippage was expected to be dominant. Figure 4(c) shows the loss modulus results for clay-*g*-PLL02/PL, which also confirms the nonterminal behavior and plasticizing behavior of clay-*g*-PLL02 mentioned above. Figure 4(a) shows a large enhancement of the shear thinning of clay-*g*-PLL02/PL at a clay content of 3 wt %. This result can be attributed to both the end-tethered effect of clay-*g*-PLL02 in the lower-frequency region and the plasticizing effect of grafted PLL chains in the higher-frequency region.

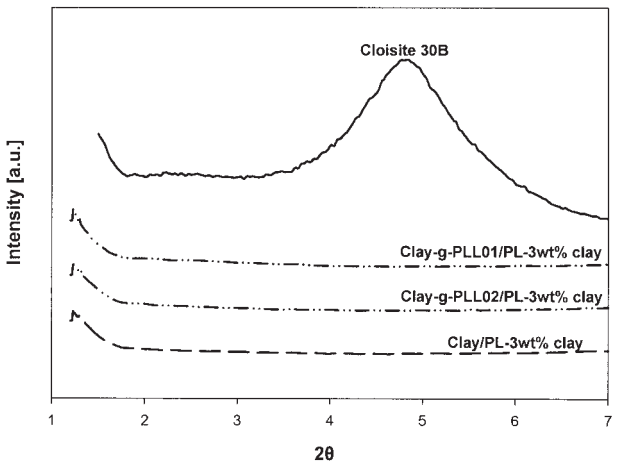

Figure 2 WAXD patterns of clay-*g*-PLL/PL and clay/PL nanocomposite (3 wt % clay): (a) clay-*g*-PLL01/PL, (b) clay-*g*-PLL02/PL, (c) clay/PL.

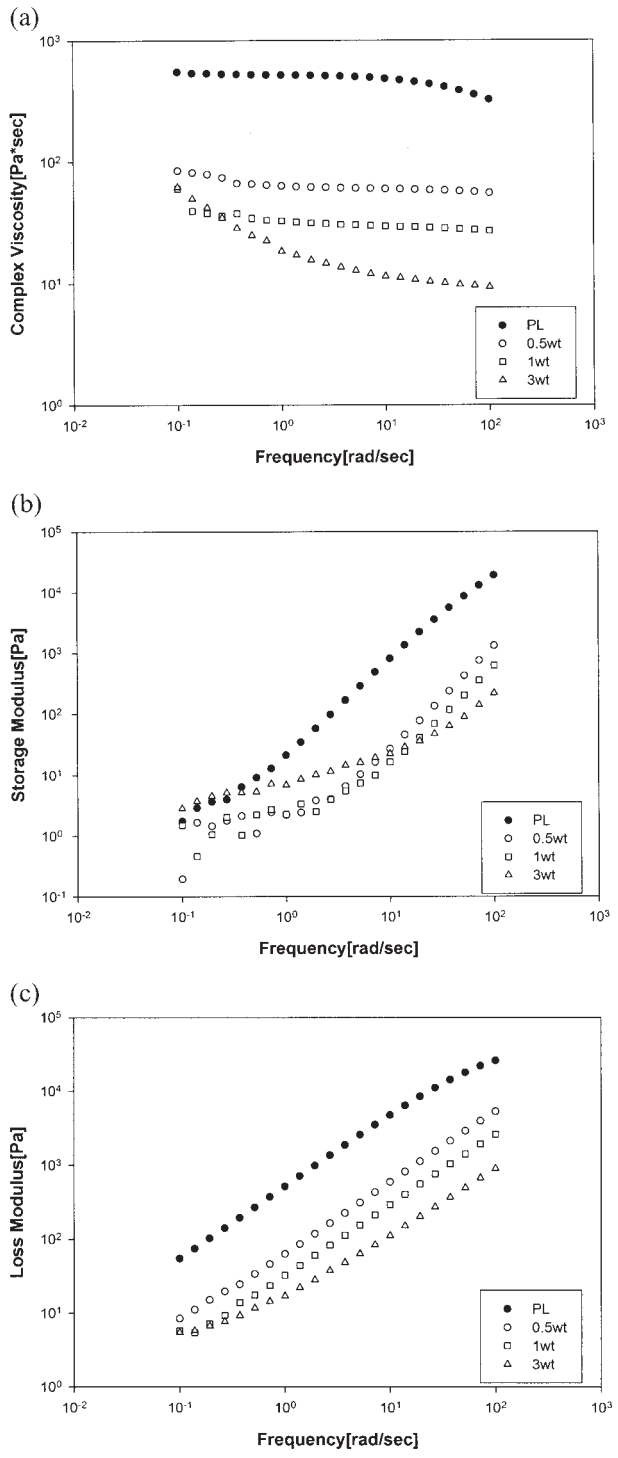

Figure 3 Rheological properties of clay-*g*-PLL01/PL at 210°C: (a) complex viscosity, (b) loss modulus, (c) storage modulus.

Rheological property of clay/PL

Figure 5 shows the complex viscosity of clay/PL, clay-*g*-PLL01/PL, and clay-*g*-PLL02/PL at a 3 wt % clay content. The shear thinning of clay/PL was found to be much less significant than in clay-*g*-PLL02/PL. This is because the effect of viscosity enhancement on complex viscosity was less significant for the nonmodified clay/PL composite. The plasticizing effect of clay-*g*-PLL02 at higher frequencies also could have contributed to the higher shear thinning. It also was shown that the complex viscosity of clay-*g*-PLL01/PL was

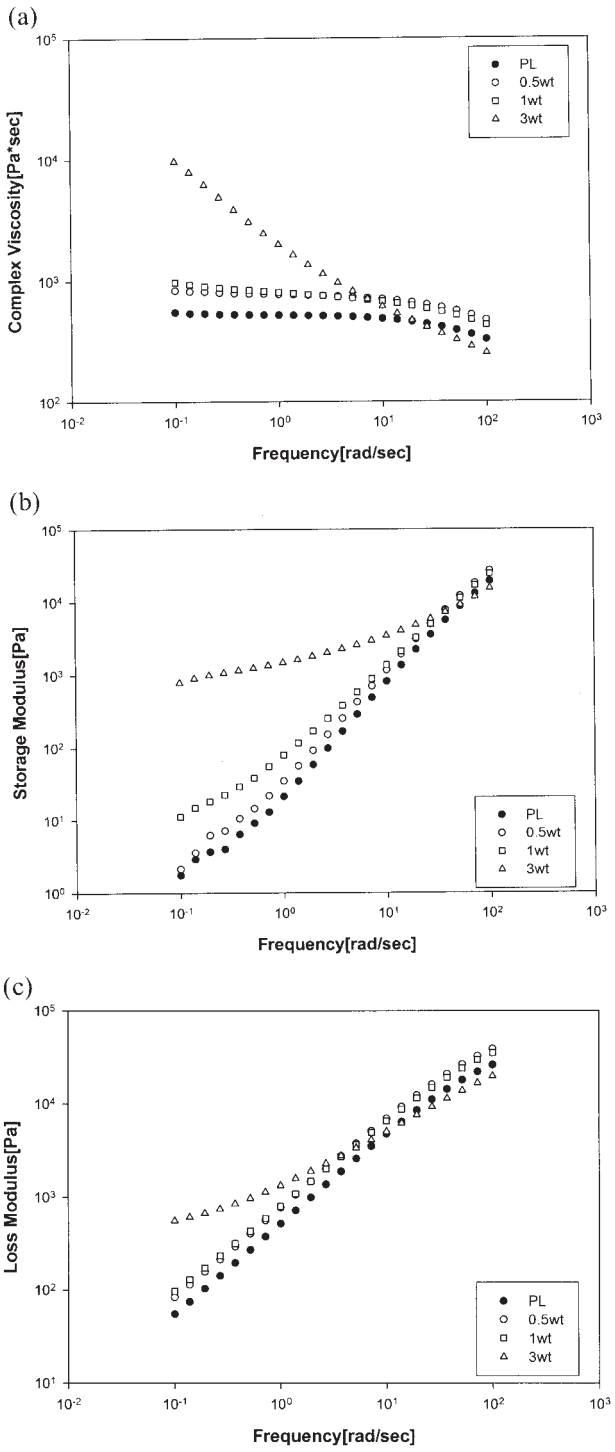

Figure 4 Rheological properties of clay-*g*-PLL02/PL at 210°C: (a) complex viscosity, (b) loss modulus, (c) storage modulus.

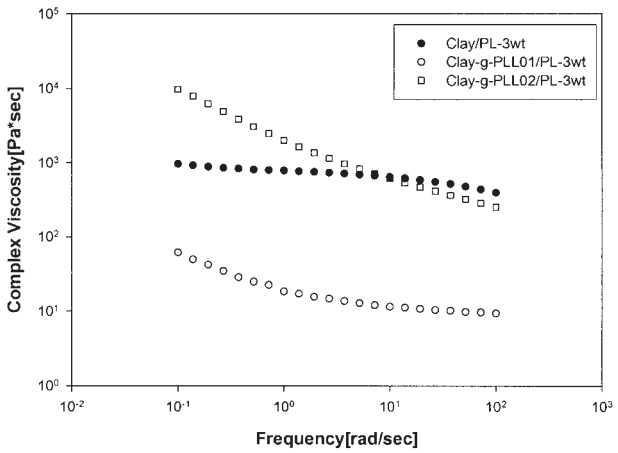

Figure 5 Complex viscosity of clay/PL, clay-*g*-PLL01/PL, and clay-*g*-PLL02/PL at 210°C (3 wt % clay).

lower than that of clay/PL. This is because of the high plasticizing effect of the short chain length of grafted PLL.

CONCLUSIONS

We prepared a novel clay/polylactide nanocomposite by introducing a modified clay into the nanocomposite and then evaluated its processability. The clay-*g*-PLL could be both an internal plasticizer and/or a viscosity enhancer depending on the molecular weight of the grafted PLL chain. When the molecular weight of the PLL grafted onto the clay surface was greater than the critical molecular weight of chain entanglement, the viscosity-enhancing effect was dominant in the low-frequency range, whereas the plasticizing effect was dominant in the high-frequency range. This led to the nanocomposite having high shear-thinning behavior. When the molecular weight of the grafted PLL was below the critical molecular weight of chain entanglement, only the plasticizing effect was apparent.

In summary, the novel clay/polylactide nanocomposite showed improved processability compared with the simply modified clay/polylactide nanocomposite.

References

1. Chasin, M.; Langer, R., Eds. Biodegradable Polymers as Drug Delivery Systems; Marcel Dekker: New York, 1990.
2. Langer, R.; Vacanti, J. P. Science 1993, 260, 920.
3. Eling, B.; Golgolewski, S.; Pennings, A. J. Polym 1982, 23, 1587.
4. Billot, J. P.; Douy, A.; Gallot, B. Makromol Chem 1976, 177, 1889.
5. Dorgan, J. R.; Lehermeier, H.; Mang, M. J Polym Environ 2000, 8, 1.
6. Yuan, X.; Mak, A. F. T.; Kwok, K. W.; Yung, B. K. O.; Yao, K. J Appl Polym Sci 2001, 81, 251.
7. Ogata, N.; Jimenez, G.; Kawai, H.; Ogihara, T. J Polym Sci, Polym Phys 1997, 35, 389.
8. Ray, S. S.; Maiti, K. P.; Okamoto, M.; Yamada, K.; Ueda, K. Macromol 2002, 35, 3104.
9. Pail, M.-A.; Alexandre, M.; Degee, P.; Calberg, C.; Jerome, R.; Dubois, P. Macromol Rapid Commun 2003, 24, 561.
10. Krishnamoorti, R.; Giannelis, E. P. Macromol 1997, 30, 4097.
11. Kricheldorf, H. R.; Kreiser-Saunders, I.; Boettcher, C. Polym 1995, 36, 1253.
12. Ray, S. S.; Yamada, K.; Okamoto, M.; Fujimoto, Y.; Ogami, A.; Ueda, K. Polym 2003, 44, 6633.
13. Lepoittevin, B.; Pantoustier, N.; Devalckenaere, M.; Alexandre, M.; Calberg, C.; Jerome, R.; Henrist, C.; Rulmont, A.; Dubois, P. Polym 2003, 44, 2033.
14. Lee, K. M.; Han, C. D. Macromol 2003, 36, 7165.
15. Dorgan, J. R.; Lehermeier, H. J.; Knauss, D.; Mang, M. Society of Rheology 71st Annual Meeting 1999; Paper MS18.
16. Dorgan, J. R.; Williams, J. S. J Rheol 1999, 43, 1141.
17. Grijpma, D. W.; Penning, J. P.; Pennings, A. J. Colloid Polym Sci 1994, 272, 1068.